

(HUANJING KEXUE)

ENVIRONMENTAL SCIENCE





₩ 姥 # 享 (HUANJING KEXUE)

ENVIRONMENTAL SCIENCE

第37卷 第2期 2016年2月15日

目 次

编者按	(403)
我国化学品的风险评价及风险管理 王铁宇,周云桥,李奇锋,吕永龙((404)
土地利用回归模型在大气污染时空分异研究中的应用 吴健生,谢舞丹,李嘉诚((413)
中国 2000 ~ 2010 年生态足迹变化特征及影响因素 黄宝荣,崔书红,李颖明((420)
关中地区冬季 PM _{2.5} 中碳气溶胶的污染特征及来源解析 田鹏山,曹军骥,韩永明,张宁宁,张蓉,刘随心((427)
利用 SPAMS 研究南宁市冬季单颗粒气溶胶化学成分 ·····	(/
刘慧琳,宋红军,陈志明,黄炯丽,杨俊超,毛敬英,李宏姣,梁桂云,莫招育((434)
南言頁季市区 VOC。特征及 O 开始满执的相关种公析。	(+5+)
南京夏季市区 VOCs 特征及 O ₃ 生成潜势的相关性分析	(112)
	(443)
北京城区气传花粉季节特征及与气象条件关系 孟龄,王效科,欧阳志云,任玉芬,王巧环((452)
里庆印垃圾煲烷)水的分种特征与人气水排放因于研究	(459)
重庆市垃圾焚烧厂汞的分布特征与大气汞排放因子研究	(466)
长沙近地面水汽中稳定同位素的监测与分析	(475)
青藏高原内陆典型冰川区"冰川-径流"汞传输过程 孙学军,王康,郭军明,康世昌,张国帅,黄杰,丛志远,张强弓((482)
西藏湖泊沉积物重金属元素特征及生态风险评估 ···················· 郭淡汐,刘勇勤,张凡,侯居峙,张宏波(坦噶尼喀湖东北部入湖河流沉积物重金属分布特征与生态风险评价 ················· 余成,陈爽,张路((490)
坦噶尼喀湖东北部入湖河流沉积物重金属分布特征与生态风险评价 余成,陈爽,张路((499)
近百年来新疆博斯腾湖多环芳烃的组成及变化特征	(507)
舟山青浜岛不同环境介质中 PAHs 的分布特征 ············ 郑煌, 邢新丽, 顾延生, 桂福坤, 祁士华, 黄焕芳 ((513)
模拟排水沟渠非点源溶质氮迁移实验研究 李强坤、宋常吉、胡亚伟、彭聪、马强、姜正曦、琚艺萌((520)
模拟排水沟渠非点源溶质氮迁移实验研究 ················ 李强坤,宋常吉,胡亚伟,彭聪,马强,姜正曦,琚艺萌(中田河流域景观异质性对水体总氮浓度影响研究 ···················· 王晶萍,李兆富,刘红玉,王刚,辛强((527)
江西香溪流域干湿季交替下底泥氮释放机制及其对流域氮输出的贡献 韩宁,郝卓,徐亚娟,高扬,于贵瑞((534)
巢湖水体氡磷营姜卦时空分布特征	(542)
巢湖水体氮磷营养盐时空分布特征 ····································	(548)
桑沟湾表层沉积物性质及对磷的吸附特征 朱佳美,曹晓燕,刘素美,王丽莎,杨桂朋,葛成凤,路敏((558)
本性行移之5000000000000000000000000000000000000	(565)
苏州市古城区降雨径流颗粒物粒径分布及污染物赋存形态 ····································	(303)
供待例有每种儿母似要架十足双共一种鬼囚了之间的相关力例 ************************************	(572)
一性序序》类##4件 cpow 中中共共体第一个 ##2+##4 开启职业 *** *** *** *** *** *** *** *** *** *	(5/3)
三峡库区消落带水体 CDOM 中电何转移配合物对具案外-可见吸収尤谱的影响	,
江稻,梁俭,张皋雪,土定男,魏世强,户松((580)
pH 对高锰酸钾氧化降解苯胺类化合物动力学的影响	(588)
EDTA 对 Pd/Fe 体系还原脱氯 2,4-D 的影响	(595)
镍铝层状氧化物薄膜电极的制备及其除盐性能 王婷,朱春山,胡承志 ((602)
微生物对砷的氧化还原竞争 杨婷婷, 柏耀辉, 梁金松, 霍旸, 王明星, 袁林江((609)
处理水产养殖污水潜流湿地中的厌氧氨氧化菌群特征 曾宪磊,刘兴国,吴宗凡,时旭,陆诗敏((615)
污水回用中主要病原菌解析及其紫外消毒效应	(622)
异养硝化-好氧反硝化菌 Burkholderia sp. YX02 强化连续流反应器中微生物群落结构解析	
一三峡库区消落带水体 CDOM 中电荷转移配合物对其紫外-可见吸收光谱的影响	(630)
基于新一代测序技术的 A ² O 与 BIOLAK 活性污泥宏基因组比较分析 田美,刘汉湖,申欣((638)
1 株海洋异养硝化-好氧反硝化菌的分离鉴定及其脱氮特性 孙庆花,于德爽,张培玉,林学政,李津((647)
纳米 Ni/Fe 用于去除染料生产废水二级生物处理出水中 AOX 和色度的研究 舒小铭,徐灿灿,刘锐,赵远,陈吕军(
3BER-S 工艺用于再生水深度脱氮同步去除 PAEs 的可行性 徐鹏程, 郝瑞霞, 张娅, 王冬月, 钟丽燕, 徐浩丹(
合成时间对钛酸盐纳米材料的影响及其吸附水中铅的性能研究 范功端,陈丽茹,林茹晶,林茜,苏昭越,林修咏	
芦苇秸秆生物炭对水中菲和1,1-二氯乙烯的吸附特性 吴晴雯,孟梁,张志豪,罗启仕,杨洁((680)
芦苇基和污泥基生物炭对水体中诺氟沙星的吸附性能 张涵瑜,王兆炜,高俊红,朱俊民,谢超然,谢晓芸。	(680)
厂 中全TH1 JVC至工物 然 A J A P P P P P P P P P P P P P P P P P	(607)
子卫生血及刀向内沿上划用沿市上横须型化影响 "你没么, 东州, 对方, 凤凰, 目既右, 与慧燕, 丁志国(横浪及红红蓝田对夕小丰田上塘城阳和横洋州的影响 ""你说,你没么, 东州, 对方, 凤凰, 目既右, 与慧燕, 丁志国((702)
季节性温度升高对落干期消落带土壤氮矿化影响 ·············· 林俊杰,张帅,刘丹,周斌,肖晓君,马慧燕,于志国(增温及秸秆施用对冬小麦田土壤呼吸和酶活性的影响 ··················· 陈书涛,桑琳,张旭,胡正华(基于 GIS 的银川市不同功能区土壤重金属污染评价及分布特征 ···························王幼奇,白一茹,王建宇((703)
基丁 GIS 的银川甲个回切能区土壤里金周万垛评价及分中特值 ·························· 土坳 奇,目一茹,土建于((/10)
不同产地硅藻土原位控制土壤镉污染差异效应与机制 朱健,王平,林艳,雷明婧,陈仰(紫色土对邻苯二甲酸二甲酯的淋溶吸持特征及影响因素 王强,宋娇艳,曾微,王法(几种修复措施对 Cd 淋失及土壤剖面运移影响 如孝利,曾昭霞,铁柏清,陈求稳,魏祥东((/1/)
家巴土对邻本—中酸—中酯的淋浴收持特征及影响因系····································	(726)
儿种修复猎酏对 Cd 淋失及土壤剖面运移影响 ····································	(734)
·····································	(740)
湿生坏境中丛枝菌根(AM)对香蒲耐 Cd 胁迫的影响 罗鹏程,李航,王曙光 ((750)
溴酸盐对水生生物的急性毒性效应 王执伟,刘冬梅,张文娟,崔福义 ((756)
自组装哑铃状 Fe ₃ O ₄ 微/纳米材料对十溴联苯的热催化降解 ····································	
一次	(765)
盐度对准好氧矿化垃圾生物反应器渗滤液处理及 N,O产生的影响 李卫华,孙英杰,刘子梁,马强,杨强((775)
污泥直接干化尾气中恶臭污染物质重要性评价: 以指标权重评分法为例	
	(782)
《环境科学》征订启事(557) 《环境科学》征稿简则(594) 信息(419,442,781)	

镍铝层状氧化物薄膜电极的制备及其除盐性能

王婷1,2,朱春山1*,胡承志2*

(1. 河南工业大学化学化工学院,郑州 450001; 2. 中国科学院生态环境研究中心,中国科学院饮用水科学与技术重点实验室,北京 100085)

摘要:水滑石不仅是一种重要的水处理吸附剂,而且在超级电容器方面有广泛应用.本研究采用原位生长法,由泡沫镍作为基体并提供镍源,在泡沫镍表面合成了镍铝复合氧化物(NiAl-MMO)薄膜即类水滑石煅烧产物.所制得的 NiAl-MMO 薄膜电极的电化学性质稳定、电容量高,此薄膜电极的单位质量的比电容量可高达 667 F·g⁻¹.对此电极进行电容除盐性能研究,结果表明,增加电压和弱碱性 pH 环境有利于该电极除盐;初始浓度为 0.003 mol·L⁻¹的情况下,最佳工作条件为:电压 1.0 V、pH 值为 8,在此时除盐效率可达 58.17%.电极反接可使吸附饱和的电极材料迅速再生,脱附率可达 87.96%.本研究为废水中盐离子的去除提供了新的技术选择.

关键词:电容去离子; 电吸附; 镍铝水滑石; 镍铝氧化物; 除盐

中图分类号: X703.1 文献标识码: A 文章编号: 0250-3301(2016)02-0602-07 **DOI**: 10.13227/j. hjkx. 2016. 02.027

Preparation of NiAl-MMO Films Electrode and Its Capacitive Deionization Property

WANG Ting^{1,2}, ZHU Chun-shan^{1*}, HU Cheng-zhi^{2*}

(1. School of Chemistry and Chemical Engineering, Henan University of Technology, Zhengzhou 450001, China; 2. Key Laboratory of Drinking Water Science and Technology, Research Center for Eco-Environmental Sciences, Chinese Academy of Science, Beijing 100085, China)

Abstract: Hydrotalcites are not only considered as important absorbents in water treatment and but also widely used as super capacitor materials. In this study, NiAl metal oxide (NiAl-MMO) films, which were the calcined products of hydrotalcite-like compounds, were grown on the surface of a foam nickel by an in-situ growth method using a foam nickel substrate as the nickel source. The prepared NiAl-MMO films electrodes materials had stable electrochemical capability, remarkable electrochemical capacitor, and gave a highest specific capacitance of 667 F·g⁻¹. The desalination performance of material indicated high voltage and weakly alkaline solution were favored for desalination. A highest desalination efficiency was up to 58. 17% when the initial concentration of Cl⁻ was 0.003 mol·L⁻¹, the voltage value was 1.0 V and pH value was 8. The adsorption saturated electrodes could be rapidly regenerated with a desorption rate of 87.96% by electrodes reversion. This study provides a new choice for desalination in wastewater treatment.

Key words: capacitive deionization; electroabsorption; NiAl layered double hydroxide; NiAl metal oxide; desalination

近年来,水资源紧缺现象日益严重,工业废水处理回用、海水淡化已引起人们的高度重视[1,2]. 电容去离子(capacitive deionization, CDI)技术是一种新型的水处理技术,与传统的除盐方法如反渗透、离子交换、蒸馏、电渗析等相比具有能耗低、无二次污染、操作及维护简单等优点,在水处理脱盐方面具有广阔的应用前景[3,4]. CDI 是利用静电力的作用强制溶液中的带电离子向具有相反电荷的电极方向移动,在电极表面形成电层,使带电离子富集在电极表面,以脱除水中的盐分,而且可通过断路或电极反接就能使吸附饱和的电极材料再生[5,6]. 电极材料是 CDI 技术的研究核心,对此目前国内外研究较多的电材料是多孔炭材料,如石墨、活性炭、活性炭纤维、碳纳米管、炭气凝胶等. 这些电极材料的特点是:比表面积大、比电容高、电化学性质稳

定[7,8].

层状双金属氢氧化物(又名类水滑石,LDHs)因其具有大的比表面积,良好的化学稳定性和高的比电容值成为近年来超级电容器研究和应用的新热点^[9,10].此外,它的层板化学组成、层间阴离子种类和数量的可调控性,使 LDHs 在阴离子的吸附方面有着广泛的应用^[11~13].但 LDHs 粉体导电性差,不能直接作为电极使用,因此将 LDHs 材料制成薄膜附着在导电性良好的基体表面形成 LDHs 薄膜电极^[14,15],该电极有望成为良好的 CDI 材料^[16].

收稿日期: 2015-07-16; 修订日期: 2015-09-09

基金项目: 国家水体污染控制与治理科技重大专项(2012ZX07414-001)

作者简介:王婷(1989~),女,硕士研究生,主要研究方向为水处理 功能材料的开发和应用, E-mail;wangt0929@163.com

^{*} 通讯联系人, E-mail; zhuchunshan@ haut. edu. cn; czhu@ rcees. ac. cn

LDHs 的 化 学 组 成 式 为 $[M_{1-x}^{2+} M_x^{3+} (OH)_2]^{x+}$ $(A^{n-})_{x/n} \cdot mH_2O$,其中, M^{2+} 、 M^{3+} 是金属阳离子, M^{2+} 可以是锌、钴、镍、镁等二价离子, M^{3+} 可以是铝、铁、铬等三价离子,金属离子位于主层板上; A^{n-} 是层间阴离子;x 为三价阳离子占所有阳离子的摩尔比;m 代表层间的水分子数[17,18] . 将 LDHs 加热到一定温度,可形成稳定的复合金属氧化物 (MMO),MMO 与客体阴离子反应,部分可恢复成有序层状结构的 LDHs,此现象称为"结构记忆"效应,这是 MMO 可用于阴离子吸附的重要原因[19,20] . 本研究在前人工作的基础上将 LDHs 制成薄膜负载在导电体表面,制成电极进行电吸附脱盐研究.

本研究由泡沫镍作为基体并提供镍源,利用原位生长法,在泡沫镍表面制备了 NiAl-LDHs 薄膜电极并成功转化为 NiAl-MMO 薄膜电极,通过 SEM、XRD、FT-IR 表征了 NiAl-LDHs、NiAl-MMO 电极表面的形貌及组成,进一步利用电化学工作站测定了 NiAl-MMO 薄膜电极的电化学性能,并考察了电压、pH 等因素对电容除盐性能的影响.

1 材料与方法

1.1 实验材料和仪器

材料:泡沫镍(纯度大于99%),购于长沙力元新材料有限公司;石墨电极(固定碳含量大于98%),购于河南省焦作市东方石墨制品厂;盐酸(HCl)、硝酸(HNO₃)、无水乙醇(CH_3CH_2OH)、异丙醇铝(C_9H_{21} AlO₃)、氨水($NH_3 \cdot H_2O$)、碳酸钠($NaCO_3$)、氢氧化钠(NaOH)等均为分析纯(AR),购于国药集团化学试剂有限公司.

仪器:X 射线粉末衍射(XRD)仪(X'Pert pro,北京明卓仪器有限公司),傅里叶红外光谱(FT-IR)仪(TENSON27,BRUKER Germany),扫描电子显微镜(SEM)(SU8020,日立公司),电感耦合等离子体扫描仪(ICP-OES)(710,Agilent Technologies U.S.A),离子色谱(IC)仪(ICS-2000,Thermo U.S.A),电化学工作站(CHI660,上海辰华仪器公司).

1.2 薄膜电极的制备方法

取厚为1 mm 的泡沫镍剪切成2 cm ×3 cm 的片,随后用1%的稀盐酸超声清洗5 min,然后用去离子水超声清洗3次,再用无水乙醇清洗1次,放入60%的烘箱中烘2h备用.

将 6 g 左右的异丙醇铝加入到浓度为 0.05 mol·L⁻¹的 100 mL 的稀硝酸溶液中,搅拌 10 min,然后将其放入油浴锅中,加热到 90℃后恒温冷凝回流

大约 6 h,冷却后形成了半透明的溶胶,将溶胶放入 离心管离心 10 min,离心后会出现少许沉淀物,将这 些少许沉淀物除去,即得到了半透明的勃姆石溶胶.

将 1% 的氨水与 3. 15 g 碳酸钠溶于 20 mL 去离子水中,用其调节勃姆石溶胶的 pH 至 7. 5 左右,然后将勃姆石溶胶导入 100mL 高压反应釜中,将处理好的泡沫镍竖直插入勃姆石溶胶中,然后将反应釜放入烘箱中,在 120℃的条件下反应 48 h. 反应结束后待反应釜冷却至室温,取出泡沫镍的样品,然后用去离子水冲洗,干燥,即获得了镍基 NiAl-LDHs 薄膜电极.

把制备好的 NiAl-LDHs 薄膜电极置于马弗炉中,在 500℃下煅烧 4 h,升温速率是 5 ℃·min⁻¹,得到煅烧产物 NiAl-MMO 薄膜电极.

1.3 除盐实验

以 3 cm × 2 cm 的石墨做负极,面积相同的 NiAl-MMO 薄膜做正极,并联相同的电极两组,放入 盛有 100 mL 浓度为 0.003 mol·L⁻¹的 NaCl 溶液的 反应器中,打开直流电源,于电压 1.0 V、pH 为 7 的 条件下,电吸附 150 min,使电吸附达到平衡. 将上述石墨电极转为正极,NiAl-MMO 薄膜电极为负极,放入原溶液中,电脱附 90 min,每隔 15 min 取样 0.5 mL,稀释后用 IC 测量 Cl⁻含量. Cl⁻的去除率、吸附容量、脱附率计算公式:

$$r = [(c_0 - c_e)/c_0] \times 100\% \tag{1}$$

$$q_e = V(c_0 - c_e)/S \tag{2}$$

$$\eta = [(c_{d} - c_{e})/(c_{0} - c_{e})] \times 100\%$$
(3)

式中, c_0 、 c_e 、 c_d 分别为 Cl^- 的初始浓度、吸附平衡浓度、 $mg \cdot L^{-1}$; q_e 为平衡吸附容量、 $mg \cdot cm^{-2}$; r 为 Cl^- 的去除率,%; V 为溶液体积,L; S 有效电极面积, cm^2 ; η 为脱附率,%.

1.4 表征方法

采用 XRD(铜靶, K α 射线, λ = 0. 154 06 nm, 管电压为 40 kV,扫描速率是 5(°)·min⁻¹,扫描范围为 10°~90°)表征 NiAl-LDHs 薄膜,粉体及其煅烧后的 NiAl-MMO 薄膜的晶相结构;将 1 mg 从 NiAl-LDHs 薄膜上刮下来的粉末样品及其煅烧后的 NiAl-MMO 粉末样品分别与 100 mg 的 KBr 粉末充分混合后压片,采用 FT-IR 在 400~4 000 cm⁻¹波数范围进行定性分析;采用 SEM-EDX 对样品表面的结构、形貌和组成进行分析;采用 ICP-OES 精确测量薄膜的组成;配制 1 mol·L⁻¹的 KOH 溶液 100 mL,以 NiAl-MMO 薄膜电极作为工作电极,以 Pt 为标准电极,饱和甘汞电极为参比电极,使用电化学工作站进行循环伏安性能和充放电性能的测试;采用 IC 测量电

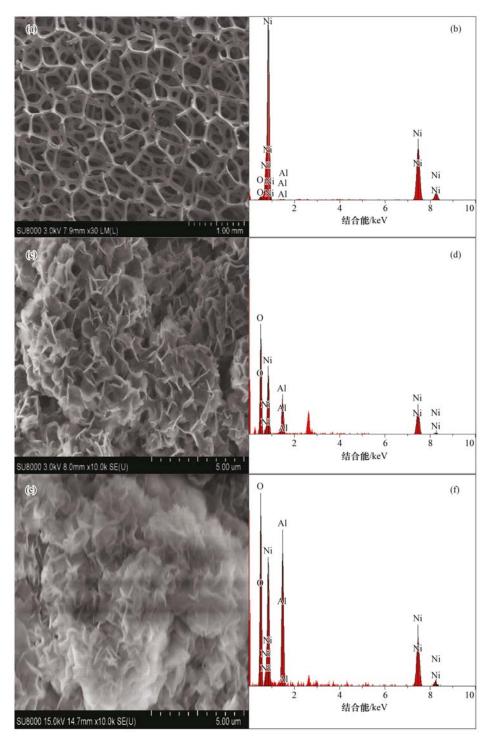
吸附及电脱附过程中的 Cl⁻变化情况.

2 结果与讨论

2.1 薄膜电极的形貌及结构 利用扫描电子显微镜(SEM)和能谱(EDX)对

泡沫镍及其表面生长的 NiAl-LDHs、NiAl-MMO 的表面形貌和组成进行表征,如图 1 所示.

图1(a)为未负载 LDHs 的空白泡沫镍电极,表面为光滑的网状结构,从图1(c)与图1(a)对比很明显看出经过原位生长法处理后的泡沫镍表面变得非常



(a)、(b)是泡沫镍的扫描电镜(SEM)图和能谱(EDX)分析图,(c)、(d)和(e)、(f)分别是 NiAl-LDHs 和 NiAl-MMO 薄膜电极的 SEM 图、EDX 图

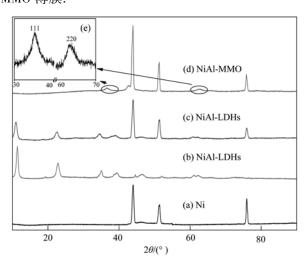
图 1 泡沫镍基体表面生长 NiAl-LDHs、NiAl-MMO 薄膜电极的 SEM 图和 EDX 图

Fig. 1 SEM images and EDX patterns of nickel foam, NiAl-LDHs films electrode and NiAl-MMO films electrode

致密,原有的网状结构被 NiAl-LDHs 薄膜覆盖,而且 NiAl-LDHs 薄膜呈现薄片堆积状态. 图 1(e)中 NiAl-MMO 薄膜仍为片状结构堆积,和 NiAl-LDHs 薄膜相比较形貌上基本没有很大变化,原因是 LDHs 脱出层间阴离子的反应主要是在层板之间进行的.

EDX 可用来分析水滑石上的镍铝含量比,EDX 数据表明 NiAl-LDHs 中镍铝的含量比为 2~4,根据 LDHs 晶体的 2价和 3价金属离子摩尔比的限定原则,只有在 2~4时才有纯的 LDHs 晶体形成^[21].为了精确确定镍铝的含量比,需要用 ICP-OES 来分析.将 NiAl-LDHs 薄膜刮下来的粉末样品溶解在硝酸中,利用 ICP-OES 测定镍铝的含量比为 2.8,两者的结果一致.

图 2 为薄膜电极在 10°~90°的 XRD 的分析结果. 图 2(b)、2(c)显示,在 11.2°、22.4°、33.6°处出现了 LDHs 的特征衍射峰(003)、(006)、(012),图 2(a)是泡沫镍的特征衍射峰,可以看到图 2(c)是图 2(a)和 2(b)的叠加,其峰的尖锐度和对称性比较好,可以说明在泡沫镍上成功地生长了 NiAl-LDHs 薄膜. 从图 2(d)可以看出,NiAl-MMO 薄膜电极的主要衍射峰是基底泡沫镍的特征峰及 43.38°氧化镍的特征峰,对 10°~40°、60°~70°范围放大观察图 2(e),可以看出在 37.18°、63.09°出现了NiAl-MMO 的特征衍射峰(111)和(220)^[22,23],由此可以说明生长的 NiAl-LDHs 薄膜已被煅烧为 NiAl-MMO 薄膜.



(a)泡沫镍; (b)NiAl-LDHs 粉体; (c)NiAl-LDHs 和(d)、(e)薄膜电极

图 2 泡沫镍、NiAl-LDHs 粉体及 NiAl-LDHs、NiAl-MMO 薄膜电极的 XRD 图

Fig. 2 XRD patterns of nickel foam, NiAl-LDHs powder, NiAl-LDHs films electrode and NiAl-MMO films electrode

图 3 是薄膜电极的 FT-IR 图. FT-IR 谱图可用来鉴定层间阴离子的种类及其层板的成键信息. 3 500 cm⁻¹附近强而宽的峰是 LDHs 层间水分子和层板上羟基伸缩振动的吸收峰; 1 650 cm⁻¹处的峰是层间水羟基 H—O—H 弯曲振动的吸收峰; 1 350 cm⁻¹处的强峰是阴离子碳酸根的(C—O)伸缩振动的吸收峰; 750 cm⁻¹处的峰是碳酸根的弯曲振动的吸收峰,说明该薄膜是碳酸根插层的 NiAl-LDHs 薄膜. 煅烧后层间的阴离子和层间的羟基脱出,得到煅烧产物 NiAl-MMO 薄膜. 从图 3 (b)中可以清楚地看出来1 350 cm⁻¹处碳酸根离子的振动峰明显减弱,1 650 cm⁻¹处层间水羟基 H—O—H 弯曲振动的吸收峰也明显减弱,说明层间的阴离子和层板的羟基经过煅烧作用后会有大量脱出^[24], NiAl-LDHs 薄膜可成功转化为 NiAl-MMO 薄膜.

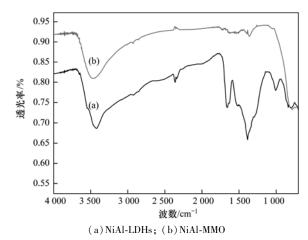


图 3 从泡沫镍上刮下来的 NiAl-LDHs 及 NiAl-MMO 的粉体的 FT-IR 图

Fig. 3 FT-IR spectra of NiAl-LDHs and NiAl-MMO powder scraped from the nickel foam substrate

2.2 电化学性能测试

利用循环伏安曲线法测试 NiAl-MMO 薄膜电极的电化学性能,扫描电压为 $0 \sim 0.45$ V,扫描速率分别为 $1 \sim 5 \sim 10$ ~ 10

图 4 为不同扫速的循环伏安曲线,与传统炭材料的双电层电容近似矩形的循环伏安曲线明显不同,图中可观察到 Ni(Ⅱ)/(Ⅲ)氧化还原反应引起的氧化还原峰,氧化还原峰的出现验证了法拉第电容的存在,发生如式(4)反应:

 $Ni(OH)_2 + OH^- = NiOOH + H_2O + e^-$ (4) 即 $Ni(II) \Longrightarrow Ni(III)$ 的电极材料化合态转移 过程^[25]. 峰电位的差值通常用于电极材料的氧化还原可逆性的表征,氧化峰与还原峰电位差值越大,表明电极材料的氧化还原可逆性越差,峰电位差值越小,表明电极材料的氧化还原可逆性越好. 由图 4 中可知在 $10 \text{ mV} \cdot \text{s}^{-1}$ 的扫速下,NiAl-MMO 的氧化峰峰电位为 0.316 V,还原峰峰电位为 0.245 V,经计算峰电位的差值为 0.069 V,和 ΔE_p 较接近,因此此电极的可逆性良好.

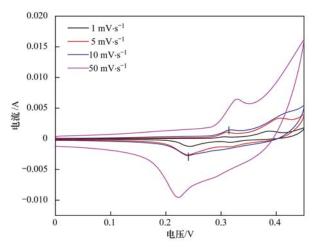


图 4 NiAl-MMO 薄膜电极的循环伏安曲线

Fig. 4 CV curves of NiAl-MMO films electrode

图 5 为不同电流密度下的充放电曲线. 由充放电曲线可以看出,放电过程由两部分组成,即快速放电阶段和电位缓慢下降阶段. 快速放电阶段由电极的内部阻抗引起,电位缓慢下降阶段中缓慢的平台则代表法拉第电容的特性. 相关研究表明法拉第电容值远远大于双电层电容值. 电容量的大小直接影响着电吸附的效能. 由图 5 充放电曲线根据比电容的计算公式(5):

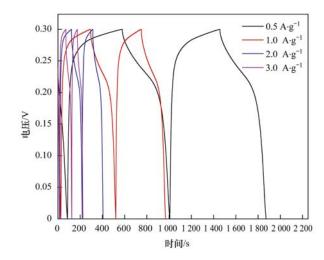
$$C_{m} = I \cdot \Delta t / \Delta V \cdot m \tag{5}$$

可以计算出样品的比电容值. 式中, C_m 表示电容,I 表示充放电电流, Δt 代表充放电时间, ΔV 代表电压,m 代表活性组分的量^[26]. 比电容量的结果如表 1 所示,可以看出随着电流密度的增大,电极放电时间减少. 这是因为电解液在较高的电流密度下,不能够与电极充分地润湿,从而减少了参与氧化还原反应的活性位点.

表 1 不同电流密度下的电容值

Table 1 Capacitance at various discharge current densities

电流密度/A·g ⁻¹	电压/V	放电时间/s	电容值/F·g ⁻¹
0. 5	0.3	400	667
1.0	0.3	180	600
2. 0	0.3	85	567
3. 0	0.3	53	530



37 卷

图 5 NiAl-MMO 薄膜电极的充放电曲线

Fig. 5 Galvanostatic charge-discharge curves of NiAl-MMO films electrode

2.3 NiAl-MMO 薄膜电极除盐性能研究

利用 NiAl-MMO 薄膜电极进行电吸附脱附性能研究. 采用 NiAl-MMO 薄膜电极电吸附 150 min 后,溶液中 Cl⁻的浓度不再减少并趋于平稳,因此选定电吸附时间为 150 min. 由图 6 可知,被 NiAl-MMO 薄膜电吸附的 Cl⁻的量为总量的 57.78%,最大吸附容量可高达 0.506 mg·cm⁻². 同样,在静态电脱附条件下,在电脱附 90 min 后,Cl⁻的浓度不再增加,因此确定电脱附时间为 90 min,Cl⁻的脱附率可达87.96%. 因此,此电极可用于废水中盐离子的电吸附脱除和回收.

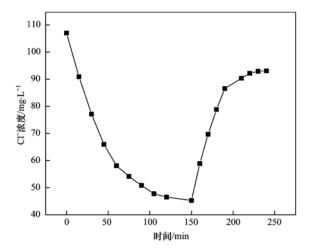


图 6 NiAl-MMO 薄膜电极的电吸附-脱附曲线

Fig. 6 Electrosorption and desorption equilibrium curve of the NiAl-MMO films electrode

图 7 是在 pH 为 7 的条件下,改变外加电压时 薄膜电极除盐效果的变化情况. 电压是决定电吸附 除盐效果的重要参数,分别在电压为 0、0.2、0.5、 0.8、1.0、1.2 V 的条件下进行除盐实验. 从中可观察到在电压为 0 V 时, NiAl-MMO 薄膜电极自身有一定的除盐效果,外加电压强化了薄膜电极的吸附效果,随着电压的升高,除盐率逐渐升高并趋于稳定. 其原因是 NiAl-MMO 薄膜电极自身就是一种稳定的阴离子吸附剂,增加电压电极表面自由电子形成的电荷密度增加,带电离子迁移到电极表面的牵引力增大,强化了薄膜电极的电吸附效果,从而提高了去除率. 当电压增大到 1.2 V 时比 1.0 V 的吸附效率并没有显著的提高,而且若再增大电压会导致水的电解,降低电流效率. 从吸附效率和能耗角度考虑,最佳工作电压应为 1.0 V.

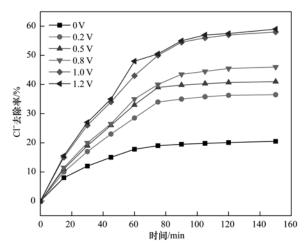


图 7 不同电压对除盐效果的影响

Fig. 7 Effect of different voltages on desalination

图 8 是电压为 1.0 V 的条件下,观察不同 pH (5、6、7、8、9)值下 NiAl-MMO 薄膜电极的除盐效果. 从中可看出当 pH 为 5 时,薄膜电极对 Cl⁻去除率最小即 30.94%,因为在酸性条件下对自身呈碱性的薄膜电极的稳定结构有损; pH 为 6~8 时,薄膜电极对 Cl⁻去除率逐渐升高,pH 为 8 时,Cl⁻的去除率达到最大即 58.17%,吸附容量为 0.510 mg·cm⁻²;当 pH 继续增大到 9 时,薄膜电极对 Cl⁻去除率为 50.13%又有所下降,因为溶液中的 OH⁻离子对 Cl⁻离子产生了竞争作用,导致薄膜电极对Cl⁻离子的吸附量下降.实验结果表明 NiAl-MMO 薄膜电极在弱碱性的条件下电吸附效果最好,在酸性和过碱性吸附效率较低.

在电压为 1.0 V、pH 为 8 的条件下,分别考察了初始 Cl^- 浓度为 0.002、0.003、0.004、0.005 $mol \cdot L^{-1}$ (71、106.5、142、177.5 $mg \cdot L^{-1}$) 时 NiAl-MMO 薄膜电极的除盐效果,实验结果如图 9 所示. 从中可以看出当浓度从 $0.002 \text{ mol} \cdot L^{-1}$ 增加到

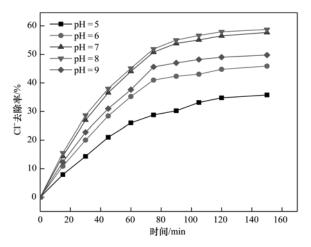


图 8 不同 pH 值对除盐效果的影响

Fig. 8 Effect of different pH value on desalination

0.005 mol·L⁻¹时,Cl⁻的去除率从59.57%下降到50.73%.说明薄膜电极除盐效率随着初始浓度的增加而降低.因为在其他条件相同的情况下,电极的吸附容量是一个定值.浓度高的溶液中所含的离子较多,在相同的时间内电极所吸附的离子就会越多,电吸附越容易达到平衡状态,所以导致除盐效率降低.

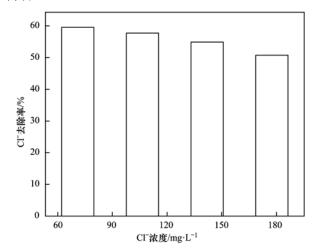


图 9 不同初始浓度对除盐效果的影响

Fig. 9 Effect of different initial concentration on desalination

3 结论

利用原位生长法,由泡沫镍作为基体并提供镍源,在泡沫镍上成功地合成了 NiAl-MMO 薄膜电极. NiAl-MMO 薄膜电极的电化学性质稳定、比电容高,在 $0.5~{\rm A\cdot g^{-1}}$ 的电流密度下比电容可达 $667~{\rm F\cdot g^{-1}}$. 初始盐浓度为 $0.003~{\rm mol\cdot L^{-1}}$ 的情况下,电压 1.0V、pH 为 $8~{\rm E}$ NiAl-MMO 薄膜电极的最佳吸附条件,对 ${\rm Cl^{-}}$ 离子的吸附率达到 58.17%,吸附容量为 $0.51~{\rm mg\cdot cm^{-2}}$. 电极反接可使 NiAl-MMO 薄膜电极脱附

再生, 脱附率可达 87.96%, 电吸附脱附简化了 NiAl-MMO 作为吸附剂的再生过程. NiAl-MMO 薄膜电极在废水中盐离子的电吸附脱除和回收方面有很大的应用前景.

参考文献:

- [1] Chen Z L, Zhang H T, Wu C X, et al. A study of electrosorption selectivity of anions by activated carbon electrodes in capacitive deionization [J]. Desalination, 2015, 369: 46-50.
- [2] Liang P, Yuan L L, Yang X F, et al. Coupling ion-exchangers with inexpensive activated carbon fiber electrodes to enhance the performance of capacitive deionization cells for domestic wastewater desalination [J]. Water Research, 2013, 47 (7): 2523-2530.
- [3] Hatzell K B, Hatzell M C, Cook K M, et al. Effect of oxidation of carbon material on suspension electrodes for flow electrode capacitive deionization [J]. Environmental Science & Technology, 2015, 49(5): 3040-3047.
- [4] Suss M E, Biesheuvel P M, Baumann T F, et al. In situ spatially and temporally resolved measurements of salt concentration between charging porous electrodes for desalination by capacitive deionization [J]. Environmental Science & Technology, 2014, 48(3): 2008-2015.
- [5] García-Quismondo E, Santos C, Lado J, et al. Optimizing the energy efficiency of capacitive deionization reactors working under real-world conditions[J]. Environmental Science & Technology, 2013, 47(20): 11866-11872.
- [6] 刘方园,胡承志,李永峰,等. MnO₂/CFP 复合电极的制备 及电吸附 Pb²⁺ 特性的研究[J]. 环境科学, 2015, **36**(2): 552-558.
- [7] 李娜, 张国珍, 杨仕超, 等. 活性炭纤维电吸附处理含盐溶液吸附特性研究[J]. 工业水处理, 2013, **33**(8): 48-51.
- [8] Kim Y J, Choi J H. Selective removal of nitrate ion using a novel composite carbon electrode in capacitive deionization [J]. Water Research, 2012, 46(18): 6033-6039.
- [9] Yan T, Zhu H Y, Li Z J, et al. Microwave synthesis of nickel/cobalt double hydroxide ultrathin flowerclusters with three-dimensional structures for high-performance supercapacitors [J]. Electrochimica Acta, 2013, 111: 71-79.
- [10] Lin W, Yu W D, Hu Z X, et al. Superior performance asymmetric supercapacitors based on flake-like Co/Al hydrotalcite and graphene[J]. Electrochimica Acta, 2014, 143: 331-339.
- [11] Zhu Y, Elzinga E J. Formation of layered Fe (II)-hydroxides during Fe (II) sorption onto clay and metal-oxide substrates [J]. Environmental Science & Technology, 2014, 48 (9): 4937-4945.
- [12] Drenkova-Tuhtan A, Mandel K, Paulus A, et al. Phosphate recovery from wastewater using engineered superparamagnetic particles modified with layered double hydroxide ion exchangers [J]. Water Research, 2013, 47(15): 5670-5677.

- [13] 钟琼, 李欢. Mg/Al 水滑石微波共沉淀法合成及其对 BrO³-吸附性能的研究[J]. 环境科学, 2014, **35**(4): 1566-1575.
- [14] Wang J, You J, Li Z S, et al. Capacitance performance of porous nickel electrode modified with Co/Al hydrotalcite [J]. Journal of Electroanalytical Chemistry, 2008, 624 (1-2): 241-244.
- [15] Yin J L, Park J Y. A nickel foam supported copper core/nickel oxide shell composite for supercapacitor applications [J]. Microporous and Mesoporous Materials, 2014, 200; 61-67.
- [16] Lei X D, Wang B, Liu J F, et al. Three-dimensional NiAl-mixed metal oxide film: preparation and capacitive deionization performances [J]. RSC Advances, 2014, 4 (78): 41642-41648.
- [17] Wu X L, Tan X L, Yang S T, et al. Coexistence of adsorption and coagulation processes of both arsenate and NOM from contaminated groundwater by nanocrystallined Mg/Al layered double hydroxides[J]. Water Research, 2013, 47(12): 4159-4168.
- [18] Lu H T, Zhu Z L, Zhang H, et al. Simultaneous removal of arsenate and antimonate in simulated and practical water samples by adsorption onto Zn/Fe layered double hydroxide [J]. Chemical Engineering Journal, 2015, 276; 365-375.
- [19] Mascolo G, Mascolo M C. On the synthesis of layered double hydroxides (LDHs) by reconstruction method based on the "memory effect" [J]. Microporous and Mesoporous Materials, 2015, 214: 246-248.
- [20] 姚铭, 杜莉珍, 王凯雄, 等. 合成水滑石治理水体阴离子染料污染研究[J]. 环境科学学报, 2005, **25**(8): 1034-1040.
- [21] Wan D J, Liu H J, Liu H P, et al. Adsorption of nitrate and nitrite from aqueous solution onto calcined (Mg-Al) hydrotalcite of different Mg/Al ratio [J]. Chemical Engineering Journal, 2012, 195-196: 241-247.
- [22] Wan D J, Liu Y D, Xiao S H, et al. Uptake fluoride from water by caclined Mg-Al-CO₃ hydrotalcite: Mg/Al ratio effect on its structure, electrical affinity and adsorptive property[J]. Colloids and Surfaces A: Physicochemical and Engineering Aspects, 2015, 469: 307-314.
- [23] 祝春蕾,王海林,孙春宝. 脱硫类水滑石衍生复合氧化物不同方法的制备与表征[J]. 环境科学,2014,35(5):2010-2017.
- [24] 王秀娟, 王海增, 孙宝维, 等. 硫氰酸根在粒状镁铝复合氧化物上的吸附性能[J]. 环境科学, 2012, **33**(9): 3182-3188.
- [25] Wang G P, Zhang L, Zhang J J. A review of electrode materials for electrochemical supercapacitors [J]. Chemical Society Reviews, 2012, 41(2): 797-828.
- [26] Hong W, Wang J Q, Niu L Y, et al. Controllable synthesis of CoAl LDH@ Ni(OH)₂ nanosheet arrays as binder-free electrode for supercapacitor applications [J]. Journal of Alloys and Compounds, 2014, 608: 297-303.

HUANJING KEXUE

Environmental Science (monthly)

Vol. 37 No. 2 Feb. 15, 2016

CONTENTS

Editor's comment · · · · · · · · · · · · · · · · · · ·	
Risk Assessment and Risk Management of Chemicals in China	WANG Tie-yu, ZHOU Yun-qiao, LI Qi-feng, et al. (404)
Application of Land-use Regression Models in Spatial-temporal Differentiation of Air Pollution	
Ecological Footprint Evolution Characteristics and Its Influencing Factors in China from 2000 to 2010	
Pollution Characteristics and Sources of Carbonaceous Aerosol in PM _{2,5} During Winter in Guanzhong Area	····· TIAN Peng-shan, CAO Jun-ji, HAN Yong-ming, et al. (427)
Chemical Composition of the Single Particle Aerosol in Winter in Nanning Using SPAMS	····· LIU Hui-lin, SONG Hong-jun, CHEN Zhi-ming, et al. (434)
Correlation Analysis Between Characteristics of VOCs and Ozone Formation Potential in Summer in Nanjing Urban District	·· YANG Xiao-xiao, TANG Li-li, ZHANG Yun-jiang, et al. (443)
Seasonal Dynamics of Airborne Pollens and Its Relationship with Meteorological Factors in Beijing Urban Area	
Mercury Distribution Characteristics and Atmospheric Mercury Emission Factors of Typical Waste Incineration Plants in Chongqing	
sector) Destinate dia management sector) Estato de Typico management de Santa de San	
Characteristics of Atmospheric Dry and Wet Deposition of Trace Metals in the Hinterland of the Three Gorges Reservoir, China · ·	
Monitoring and Analysis of Stable Isotopes of the Near Surface Water Vapor in Changsha	
Mercury Transport from Glacier to Runoff in Typical Inland Glacial Area in the Tibetan Plateau	
Characteristics and Risk Assessment of Heavy Metals in Core Sediments from Lakes of Tibet	
Distribution and Potential Ecological Risk Assessment of Heavy Metals in Surface Sediments of Inflow Rivers to Northeastern Lake	
Over One Hundred Year Sediment Record of Polycyclic Aromatic Hydrocarbons in the Lake Bosten, Xinjiang	
Distribution Characteristics of Polycyclic Aromatic Hydrocarbons in Different Environmental Media from Qingbang Island, Zhoushan	n, China
	ZHENG Huang, XING Xin-li, GU Yan-sheng, et al. (513)
Transformation of Non-point Source Soluble Nitrogen in Simulated Drainage Ditch	
Influence of Landscape Heterogeneity on Total Nitrogen Concentration in Zhongtian River Watershed	
Nitrogen Release from Sediment Under Dry and Rainy Season Alternation and Its Contribution to N Export from Xiangxi Watershed	In Jiangxi Province
Spatial and Temporal Distributions of Nitrogen and Phosphate in the Chaohu Lake	HAN Ning, HAU Zhuo, AU 1a-juan, et al. (534)
Phosphorus Fractions and Release Risk in Surface Sediments of an Agricultural Headwater Stream System in Hefei Suburban, Chin	
Prosphorus Fractions and Release Risk in Surface Sediments of an Agricultural rieadwater Stream System in rieter Suburban, Chin Surface Property and Sorption Characteristics of Phosphorus onto Surface Sediments in Sanggou Bay	
Particle Size Distribution and Pollutant Speciation Analyses of Stormwater Runoff in the Ancient Town of Suzhou	
Abundance of Toxic and Non-toxic Microcystis sp. in Lake Hongze and Its Correlation with Environmental Factors	
Effect of Charge-Transfer Complex on Ultraviolet-Visible (UV-Vis) Absorption Property of Chromophoric Dissolved Organic Matter	
Zones of the Three Gorges Reservoir Areas	
Influence of pH on Kinetics of Anilines Oxidation by Permanganate	
Effects of EDTA on the Reductive Dechlorination of 2,4-D by Pd/Fe	
Preparation of NiAl-MMO Films Electrode and Its Capacitive Deionization Property	
Competitive Microbial Oxidation and Reduction of Arsenic	······ YANG Ting-ting, BAI Yao-hui, LIANG Jin-song, et al. (609)
Community Characteristics of ANAMMOX Bacteria in Subsurface Flow Constructed Wetland (SSFCW) for Processing of Aquacultur	re Waster Water
	ZENG Xian-lei, LIU Xing-guo, WU Zong-fan, et al. (615)
Analysis of Pathogenic Bacteria in Reclaimed Water and Impact of UV Disinfection on the Removal of Pathogenic Bacteria	JING Ming, WANG Lei (622)
Analysis of the Microbial Community Structure in Continuous Flow Reactor Enhanced by Heterotrophic Nitrification and Aerobic De	enitrification Bacterium Burkholderia sp. YX02 ·····
That you we are street and the stree	······ SHAO Ji-lun, CAO Gang, LI Zi-hui, et al. (630)
Comparative Metagenomics of BIOLAK and A ² O Activated Sludge Based on Next-generation Sequencing Technology	TIAN Mei, LIU Han-hu, SHEN Xin (638)
Identification and Nitrogen Removal Characteristics of a Heterotrophic Nitrification-Aerobic Denitrification Strain Isolated from Marie	ine Environment · · · · · · · · · · · · · · · · · · ·
Total Carlotte Carlot	SUN Qing-hua, YU De-shuang, ZHANG Pei-yu, et al. (647)
Removal of AOX and Chroma in Biologically Treated Effluent of Chemical Dyestuff Wastewater with Nanoscale Ni/Fe	
Feasibility of 3BER-S Process for the Deep Denitrification in Synch with the Removal of PAEs from Reclaimed Water	XU Peng-cheng, HAO Rui-xia, ZHANG Ya, et al. (662)
Influence of Reaction Time on Titanate Nanomaterials and Its Adsorption Capability for Lead in Aqueous Solutions	
Sorption Characteristics of Phenanthrene and 1,1-Dichloroethene onto Reed Straw Biochar in Aquatic Solutions	
Adsorption Characteristics of Norfloxacin by Biochars Derived from Reed Straw and Municipal Sludge	
Effect of Seasonal Temperature Increasing on Nitrogen Mineralization in Soil of the Water Level Fluctuating Zone of Three Gorge Temperature Increasing on Nitrogen Mineralization in Soil of the Water Level Fluctuating Zone of Three Gorge Temperature Increasing on Nitrogen Mineralization in Soil of the Water Level Fluctuating Zone of Three Gorge Temperature Increasing Contract Con	ributary During the Dry Period
Effects of Warming and Straw Application on Soil Respiration and Enzyme Activity in a Winter Wheat Cropland	
Distribution of Urban Soil Heavy Metal and Pollution Evaluation in Different Functional Zones of Yinchuan City	The state of the s
Differential Effect and Mechanism of in situ Immobilization of Cadmium Contamination in Soil Using Diatomite Produced from Diffe Characteristics of Adsorption Leaching and Influencing Factors of Dimethyl Phthalate in Purple Soil	
Characteristics of Adsorption Leaching and influencing ractors of Dimetryl Phinalate in Purple Soil	
Cd Runoff Load and Soil Profile Movement After Implementation of Some Typical Contaminated Agricultural Soil Remediation Strat-	egies ·····
Cd Runoff Load and Soil Profile Movement After Implementation of Some Typical Contaminated Agricultural Soil Remediation Strategy	egies
Cd Runoff Load and Soil Profile Movement After Implementation of Some Typical Contaminated Agricultural Soil Remediation Strate Concentrations and Component Profiles PAHs in Surface Soils and Wheat Grains from the Cornfields Close to the Steel Smelting In	egies
Cd Runoff Load and Soil Profile Movement After Implementation of Some Typical Contaminated Agricultural Soil Remediation Strate Concentrations and Component Profiles PAHs in Surface Soils and Wheat Grains from the Cornfields Close to the Steel Smelting Inc.	egies
Cd Runoff Load and Soil Profile Movement After Implementation of Some Typical Contaminated Agricultural Soil Remediation Strate Concentrations and Component Profiles PAHs in Surface Soils and Wheat Grains from the Cornfields Close to the Steel Smelting Inc. Effect of Arbuscular Mycorrhiza (AM) on Tolerance of Cattail to Cd Stress in Aquatic Environment	egies
Cd Runoff Load and Soil Profile Movement After Implementation of Some Typical Contaminated Agricultural Soil Remediation Strategy Concentrations and Component Profiles PAHs in Surface Soils and Wheat Grains from the Cornfields Close to the Steel Smelting Inc. Effect of Arbuscular Mycorrhiza (AM) on Tolerance of Cattail to Cd Stress in Aquatic Environment Acute Toxic Effects of Bromate on Aquatic Organisms	egies
Cd Runoff Load and Soil Profile Movement After Implementation of Some Typical Contaminated Agricultural Soil Remediation Strate Concentrations and Component Profiles PAHs in Surface Soils and Wheat Grains from the Cornfields Close to the Steel Smelting Inc. Effect of Arbuscular Mycorrhiza (AM) on Tolerance of Cattail to Cd Stress in Aquatic Environment Acute Toxic Effects of Bromate on Aquatic Organisms Development of Self-assembled Dumbbell-like Fe ₃ O ₄ Micro/nanomaterial for Application in Thermocatalytic Degradation of Polybroment	egies
Cd Runoff Load and Soil Profile Movement After Implementation of Some Typical Contaminated Agricultural Soil Remediation Strate Concentrations and Component Profiles PAHs in Surface Soils and Wheat Grains from the Cornfields Close to the Steel Smelting Inc. Effect of Arbuscular Mycorrhiza (AM) on Tolerance of Cattail to Cd Stress in Aquatic Environment Acute Toxic Effects of Bromate on Aquatic Organisms Development of Self-assembled Dumbbell-like Fe ₃ O ₄ Micro/nanomaterial for Application in Thermocatalytic Degradation of Polybromatory (Contaminated Agricultural Soil Remediation Strategy (Contaminated A	egies
Cd Runoff Load and Soil Profile Movement After Implementation of Some Typical Contaminated Agricultural Soil Remediation Strates. Concentrations and Component Profiles PAHs in Surface Soils and Wheat Grains from the Cornfields Close to the Steel Smelting Inc. Effect of Arbuscular Mycorrhiza (AM) on Tolerance of Cattail to Cd Stress in Aquatic Environment Acute Toxic Effects of Bromate on Aquatic Organisms Development of Self-assembled Dumbbell-like Fe ₃ 0 ₄ Micro/nanomaterial for Application in Thermocatalytic Degradation of Polybromator of Salinity on Leachate Treatment and N ₂ 0 Releases from Semi-aerobic Aged-refuse Bioreactor Evaluating the Significance of Odor Gas Released During the Directly Drying Process of Sludge: Based on the Multi-index Integrate	egies
Cd Runoff Load and Soil Profile Movement After Implementation of Some Typical Contaminated Agricultural Soil Remediation Strate Concentrations and Component Profiles PAHs in Surface Soils and Wheat Grains from the Cornfields Close to the Steel Smelling Inc. Effect of Arbuscular Mycorrhiza (AM) on Tolerance of Cattail to Cd Stress in Aquatic Environment Acute Toxic Effects of Bromate on Aquatic Organisms Development of Self-assembled Dumbbell-like Fe ₃ O ₄ Micro/nanomaterial for Application in Thermocatalytic Degradation of Polybromatory and the Control of Self-assembled Dumbbell-like Fe ₃ O ₄ Micro/nanomaterial for Application in Thermocatalytic Degradation of Polybromatory and the Control of Self-assembled Dumbbell-like Fe ₃ O ₄ Micro/nanomaterial for Application in Thermocatalytic Degradation of Polybromatory and the Control of Self-assembled Dumbbell-like Fe ₃ O ₄ Micro/nanomaterial for Application in Thermocatalytic Degradation of Polybromatory and the Control of Self-assembled Dumbbell-like Fe ₃ O ₄ Micro/nanomaterial for Application in Thermocatalytic Degradation of Polybromatory and the Control of Self-assembled Dumbbell-like Fe ₃ O ₄ Micro/nanomaterial for Application in Thermocatalytic Degradation of Polybromatory and the Control of Self-assembled Dumbbell-like Fe ₃ O ₄ Micro/nanomaterial for Application in Thermocatalytic Degradation of Polybromatory and the Control of Self-assembled Dumbbell-like Fe ₃ O ₄ Micro/nanomaterial for Application in Thermocatalytic Degradation of Polybromatory and the Control of Self-assembled Dumbbell-like Fe ₃ O ₄ Micro/nanomaterial for Application in Thermocatalytic Degradation of Polybromatory and the Control of Self-assembled Dumbbell-like Fe ₃ O ₄ Micro/nanomaterial for Application in Thermocatalytic Degradation of Polybromatory and the Control of Self-assembled Dumbbell-like Fe ₃ O ₄ Micro/nanomaterial for Application in Thermocatalytic Degradation of Polybromatory and Degradation of Polybromatory and Degradation of Polybromatory and Degradation of Poly	egies

《环境科学》第6届编辑委员会

主 编:欧阳自远

副主编:赵景柱 郝吉明 田 刚

编 委:(按姓氏笔画排序)

万国江 王华聪 王凯军 王绪绪 田 刚 田 静 史培军

朱永官 刘志培 刘 毅 汤鸿霄 孟 伟 周宗灿 林金明

欧阳自远 赵景柱 姜 林 郝郑平 郝吉明 聂永丰 黄 霞

黄耀 鲍强潘纲潘涛魏复盛

环维种草

(HUANJING KEXUE)

(月刊 1976年8月创刊)

2016年2月15日 第37卷 第2期

ENVIRONMENTAL SCIENCE

(Monthly Started in 1976)

Vol. 37 No. 2 Feb. 15, 2016

	2010	127119 11 7137 12 71277			
主	管	中国科学院	Superintended	by	Chinese Academy of Sciences
主	办	中国科学院生态环境研究中心	Sponsored	by	Research Center for Eco-Environmental Sciences, Chinese
协	办	(以参加先后为序)			Academy of Sciences
		北京市环境保护科学研究院	Co-Sponsored	by	Beijing Municipal Research Institute of Environmental
		清华大学环境学院			Protection
主	编	欧阳自远			School of Environment, Tsinghua University
编	辑	《环境科学》编辑委员会	Editor-in -Chief		OUYANG Zi-yuan
210	14	北京市 2871 信箱(海淀区双清路	Edited	by	The Editorial Board of Environmental Science (HUANJING
		18号,邮政编码:100085)			KEXUE)
		电话:010-62941102,010-62849343			P. O. Box 2871, Beijing 100085, China
		传真:010-62849343			Tel:010-62941102,010-62849343; Fax:010-62849343
		E-mail; hjkx@ rcees. ac. cn			E-mail:hjkx@ rcees. ac. cn
		http://www.hjkx.ac.cn			http://www. hjkx. ac. en
出	版	舒学出版社	Published	by	Science Press
_		北京东黄城根北街 16 号			16 Donghuangchenggen North Street,
		邮政编码:100717			Beijing 100717, China
印刷装	き订	北京北林印刷厂	Printed	by	Beijing Bei Lin Printing House
发	行	斜华出版社	Distributed	by	Science Press
		电话:010-64017032			Tel:010-64017032
		E-mail:journal@mail.sciencep.com			E-mail:journal@mail.sciencep.com
订 购	处	全国各地邮电局	Domestic		All Local Post Offices in China
国外总统	发行	中国国际图书贸易总公司	Foreign		China International Book Trading Corporation (Guoji
		(北京 399 信箱)			Shudian), P. O. Box 399, Beijing 100044, China

中国标准刊号: ISSN 0250-3301 CN 11-1895/X

国内邮发代号: 2-821

国内定价:120.00元

国外发行代号: M 205

国内外公开发行